MODELING THE AUTO IGNITION OF COMBUSTIBLE FLUID IN INSULATION MATERIALS INCORPORATING PARTIAL PRESSURE OF THE VAPOUR AND HEAT TRANSFER AT THE SURFACE

GIMBA, A. S., & OLAYIWALA, R. O.
Department of Mathematics,
Federal University of Technology, Minna, Nigeria
E-mail: asgimba000@gmail.com; olayiwola.rasaq@futminna.edu.ng
Phone: +234-706-323-3364

Abstract
This paper presents an approximate analytical solution capable of predicting the concentration, temperature and partial pressure distributions in a process of auto ignition of combustible fluids in insulation materials incorporating heat transfer at the surface. The analytical solution is obtained via polynomial approximation method, which show the influence of the parameters involved on the system. The effect of change in parameters such as the Frank-Kamenetskii number and the endothermicity, Nusselt and Lewis numbers are presented graphically and discussed. The results obtained revealed that Frank-Kamenetskii and Nusselt numbers enhanced the medium temperature and oxygen concentration while it decreases the fluid concentration and partial pressure of vapour.

Keywords: Auto-ignition, Combustible fluids, Heat transfer at the surface, Polynomial approximation method.

Introduction

Stringent emissions regulations and significant increases in fuel prices are having a marked effect on the growth rate of automotive technology development with the objective of reducing fuel consumption and improving engine efficiency (Kamil *et al., 2014)*. Controlled auto-ignition based combustion systems such as homogeneous charge compression ignition (HCCI) (Aziz *et al.,* 2013), stratified charge combustion ignition (SCCI) (Chen *et al.,* 2006) premixed charge compression ignition (PCCI) (Kocher *et al., 2014*), and reactivity charge compression ignition (RCCI) (Firmansyah *et al.,* 2013) are recent engine developments with high efficiency, and low emissions and fuel consumption.

These combustion systems are proven to be able to significantly reduce the fuel consumption and exhaust emission, but with drawbacks in performance and operating range. The fuel type is the most significant parameter in the auto-ignition behavior of a mixture (Krasselt *et* al., 2013) in controlled auto-ignition based combustion systems such as HCCI. A significant number of experiments and simulations aimed at improving the understanding of the auto-ignition process have been carried out (Lu *et al*., 2006). Furthermore, most of these investigations used a primary reference fuel (PRF) composition that had similar ignition delay properties to those of commercial fuel in order to get a better understanding of the auto-ignition process (Saxena *et al*., 2013).

What others have done

Beever *et al.* (1994), demonstrated experimentally the phenomenon of autoignition of combustible fluids in porous insulation materials and established a simple theoretical model for the onset of thermal runaway, including a modified definition of ignition. Their model equations are

Energy Equation

$$\rho_s' c_{ps}' \frac{dT}{dt'} = \rho_a' \left(\frac{\rho_{0_2}'}{\rho_a'}\right)\left(\frac{\rho_L'}{\rho_a'}\right)\left(\frac{\Delta H_{oxid}'}{Woxid}\right) \times A' e^{-\frac{E}{R'T'}} - \frac{h'S'}{V'}(T' - T_a') - \rho_L^1 \left(\frac{\Delta H_L'}{W_L'}\right) F' e^{-\frac{T_P'}{T}} \quad (1)$$

Oxidation Heat transfer at the surface Evaporation

Combustible Fluid

$$\rho_s' c_{ps}' \frac{d\rho_L'}{dt'} = -\rho_a' F' e^{-\frac{T_P'}{T'}} - \rho_L' \left(\frac{\rho_{0_2}'}{\rho_a'}\right) \times A' e^{-\frac{E}{R'T'}} \quad (2)$$

Evaporation Oxidation

Where standard notation is used for enthalpy $\Delta H'$, temperature T', activation energy (E') density (p'), specific heat (c_p'), surface area s', and Volume (V'). The subscripts O_2 and (L) refer to as oxygen and the combustible liquid, respectively and all dashed quantities are dimensional. The remaining terms represent heat transfer coefficient (h^1), reaction frequencies $(F' \quad A')$, ambient temperature (T_a') and the temperature coefficient for evaporation (T_v').

The objectives of this study are to:

(i) Formulate one dimensional equation governing the phenomenon.
(ii) Obtain the analytical solution using polynomial approximation method
(iii) Provide the graphical representation of the system responses

Model Formulation

Here, the work of Olayiwala *et al*. (2019) is extended by incorporating partial pressure of vapour and heat transfer at the surface.

The respective conservation equations governing the phenomena are;

$$\frac{\partial T}{\partial t} = \frac{k}{\rho c r^2}\frac{\partial}{\partial r}\left(r^2 \frac{\partial T}{\partial r}\right) + \frac{QA}{\rho c} C_f^{\alpha} C_{ox}^{\beta} e^{-\frac{E}{RT}} - \frac{Q_v F}{\rho c} C_f e^{-\frac{E_v}{RT}} - \frac{hs}{\rho c v}(T - T_a) \quad (3)$$

$$\frac{\partial C_f}{\partial t} = \frac{D_f}{r^2}\frac{\partial}{\partial r}\left(r^2 \frac{\partial C_f}{\partial r}\right) - A C_f^{\alpha} C_{ox}^{\beta} e^{-\frac{E}{RT}} - F C_f e^{-\frac{E_v}{RT}} \quad (4)$$

$$\frac{\partial C_{ox}}{\partial t} = \frac{D_0}{r^2}\frac{\partial}{\partial r}\left(r^2 \frac{\partial C_{ox}}{\partial r}\right) - v A C_f^{\alpha} C_{ox}^{\beta} e^{-\frac{E}{RT}} \quad (5)$$

$$\frac{\partial p}{\partial t} = \frac{D_v}{r^2}\frac{\partial}{\partial r}\left(r^2 \frac{\partial p}{\partial r}\right) + \frac{RT}{\gamma m p} F C_f e^{-\frac{E_v}{RT}} \quad (6)$$

With the initial and boundary condition:

$$\left.\begin{array}{l} T(r,0)=T_0, \quad \left.\frac{\partial T}{\partial r}\right|_{r=0}=0, \quad K^*\left.\frac{\partial T}{\partial r}\right|_{r=r_0}=h(T_0-T|_{r=r_0}) \\ \mathrm{C}_f(r,0)=\mathrm{C}_{f_0}, \quad \left.\frac{\partial \mathrm{C}_f}{\partial r}\right|_{r=0}=0, \quad \mathrm{D}_f^*\left.\frac{\partial \mathrm{C}_f}{\partial r}\right|_{r=r_0}=-K_{mf}(\mathrm{C}_{f_0}+\mathrm{C}_f|_{r=r_0}) \\ \mathrm{C}_{ox}(r,0)=\mathrm{C}_{ox0}, \quad \left.\frac{\partial \mathrm{C}_{ox}}{\partial r}\right|_{r=0}=0, \quad \mathrm{D}_0^*\left.\frac{\partial \mathrm{C}_{ox}}{\partial r}\right|_{r=r_0}=-K_{mox}(\mathrm{C}_{ox0}+\mathrm{C}_{ox}|_{r=r_0}) \\ \mathrm{P}(r,0)=P_0, \quad \left.\frac{\partial P}{\partial r}\right|_{r=0}=0, \quad \mathrm{D}_v^*\left.\frac{\partial P}{\partial r}\right|_{r=r_0}=q(\mathrm{P}_0-P|_{r=r_0}) \end{array}\right] \tag{7}$$

Where

C_{ox} is the concentration of oxygen , C_f is the concentration of condensed reactant, D_0 is the oxygen diffusion coefficient, D_f is the condense reactant diffusion coefficient , ρ is the density of the reactant, p_0 is standard pressure, k is the thermal conductivity of the medium , c is the heat capacity of the medium, Q is the enthalpy of oxidation (exothermicity), Q_v is the enthalpy of vaporization (endothermicity), R is the universal gas constant, T is the temperature of the medium , E is the activation energy (reaction), E_{va} is the activation energy (vaporization), T_0 is the initial temperature of the medium, V is the stoichiometry coefficient, C_{ox0} is the initial oxygen concentration within the insulation black, c_{f0} is the initial concentration of the uniformly distributed fluid, t is the time, A is the pre-exponent factor (reaction), F is the pre-exponent factor (vaporization), α and β are the order of reaction , r is the spatial coordinate, D_0^* is the effective oxygen diffusion coefficient , D_f^* is the effective condensed reactant diffusion coefficient D_v is the diffusion coefficient for vapour, D_v^* is the effective diffusion coefficient, k^* is the effective thermal conductivity of the medium, k_{mf} is the condensed reactant convective mass transfer coefficient , K_{mox} is the oxygen convective mass transfer coefficient, h is the convective heat transfer coefficient, hT_0 is the heat energy released per unit time by the reaction $h|_r$ is the energy flux induced by the motion of the boundary energy conservation $k_{mf}c_{cf_0}$ is the number of mole per unite time of condensed fluid , $k_{mf}|_r$ is the mass flux of condensed fluid induced by the motion of the boundary preserve mass conservation $k_{mox}c_{ox0}$ is the number of moles per unit time of oxidizer that diffused into the system for the reaction, $k_{mox}c_{ox0}r$ is the mass flux of oxidizer.

Method of Solution
Non-dimensionlisation

Dimensionless variable for space and time is been introduce as:

$$r' = \frac{r}{r_0}, \qquad t' = \frac{D_f t}{r_0^2} \tag{8}$$

Dimensionless variable for medium temperature, condensed fluid concentration, oxygen concentration and partial pressure of the vapour are been introduced as follows:

$$\theta = \frac{E}{RT_0^2}\left(T - T_0\right), \quad \psi = \frac{C_f}{C_{f_0}}, \quad \phi = \frac{C_{ox}}{C_{ox0},}, \quad p' = \frac{p}{p_0}, \quad E_v = nE, \quad \in = \frac{RT_0}{E} \qquad (9)$$

Using (8) and (9), and after dropping the prime, equation (3)-(7) become.

$$\frac{\partial \theta}{\partial t} = \frac{Le}{r^2}\frac{\partial}{\partial r}\left(r^2 \frac{\partial \theta}{\partial r}\right) - \sigma(\theta + a^*) + \delta \psi^{\alpha}\phi^{\beta} e^{-\frac{\theta}{1+\in\theta}} - \delta_v \psi e^{\frac{n\theta}{1+\in\theta}} \qquad (10)$$

$$\frac{\partial \psi}{\partial t} = \frac{1}{r^2}\frac{\partial}{\partial r}\left(r^2 \frac{\partial \psi}{\partial r}\right) - \sigma_1 \psi^{\alpha}\phi^{\beta} e^{\frac{n\theta}{1+\in\theta}} - \sigma_2 \psi e^{-\frac{n\theta}{1+\in\theta}} \qquad (11)$$

$$\frac{\partial \phi}{\partial t} = \frac{\sigma_4}{r^2}\frac{\partial}{\partial r}\left(r^2 \frac{\partial \phi}{\partial r}\right) - \sigma_5 \psi^{\alpha}\phi^{\beta} e^{\frac{\theta}{1+\in\theta}} \qquad (12)$$

$$\frac{\partial p}{\partial t} = \frac{\sigma_3}{r^2}\frac{\partial}{\partial r}\left(r^2 \frac{\partial p}{\partial r}\right) + \sigma_6 \psi e^{\frac{\theta}{1+\in\theta}} \qquad (13)$$

$$\left.\begin{array}{llll}
\theta(r,0) = 0 & \left.\frac{\partial \theta}{\partial r}\right|_{r=0} = 0 & \left.\frac{\partial \theta}{\partial r}\right|_{r=0} = -Nu\,\theta\big|_{r'=1} \\
\psi(r,0) = 1 & \left.\frac{\partial \psi}{\partial r}\right|_{r=0} = 0 & \left.\frac{\partial \psi}{\partial r}\right|_{r=1} = -sh_1\psi\big|_{r=1} \\
\phi(r,0) = 1 & \left.\frac{\partial \phi}{\partial r}\right|_{r=0} = 0 & \left.\frac{\partial \phi}{\partial r}\right|_{r=1} = -sh_2\phi\big|_{r=1} \\
\left.\frac{\partial p}{\partial r}\right|_{r=0} = 0 & \left.\frac{\partial p}{\partial r}\right|_{r=0} = 0 & \left.\frac{\partial p}{\partial r}\right|_{r=1} = -sh_3 p\big|_{r=1}
\end{array}\right], \qquad (14)$$

Where

$Le = \frac{K}{\rho c D_f}$ is the Lewis number , $\sigma = \frac{hsr_0^2}{\rho cv D_f}$, $\delta = \frac{QAr_0^2 C_{f0}^{\alpha} C_{ox0}^{\beta} e^{-\frac{E}{RT_0}}}{\rho c \in T_0 D_f}$ is the Frank-Kamenetskii number(reaction), $\delta_v = \frac{Q_v Fr_0^2 C_{f0} e^{-\frac{nE}{RT_0}}}{\rho c \in T_0 D_f}$ is the Frank-Kamenetskii number(Vaporization), $a^* = \frac{T_0 - T_a}{\in T_0}$, $\sigma_1 = \frac{Ar_0^2 CF_0^{\alpha} C_o x_0^{\ \beta}}{D_f C_{f_0}} e^{-\frac{E}{RT_0}}$, $\sigma_2 = \frac{r_0^2 C_{f_0}}{D_f C_{f_0}} e^{-\frac{nE}{RT_0}}$, $\sigma_4 = \frac{C_{ox0} D_0}{r^2 D_f C_{ox0}}$,

$$\sigma_5 = \frac{VAr_0^2 C_{f_0}^{\alpha} C_{ox0}^{\ \ \beta} e^{-\frac{E}{RT_0}}}{C_{ox0} D_F}$$

Analytical Solution by Polynomial Approximation Method

Using polynomial approximation method, the approximate analytical solution of the question (10)-(14) is obtained as:

$$\theta(r,t)=\mathrm{A}e^{-ut}-Be^{-ut}r^2+\in\begin{pmatrix} E_1e^{-F.t}-E_2(1-e^{-F_0t})+E_3(e^{-(\alpha v+\beta w)}-e^{-F_0t}) \\ +E_4(e^{-(\mathrm{u}+\alpha v+\beta w)}-e^{-F_0t})+E_5(e^{-(\mathrm{u}+v)}-e^{-F_0t})+\mathrm{E}_6((e^{-F.t})+ \\ E_7(1-e^{-F_0t})-E_8(e^{-(\alpha v+\beta w)}-e^{-F_0t})-E_9(e^{-(\mathrm{u}+\alpha v+\beta w)}-e^{-F_0t}) \\ -E_{10}(e^{-(\mathrm{u}+v)}-e^{-F_0t}))\,\mathrm{r}^2 \end{pmatrix} \quad (15)$$

$$\psi(r,t)=\mathrm{A}_1e^{-vt}-B_1e^{-vt}r^2+\in\begin{pmatrix} H_1(e^{-(\alpha v+\beta w)}-e^{-G_0t}) \\ +H_2(e^{-(\mathrm{u}+\alpha v+\beta w)}-e^{-G_0t})+H_3(e^{-(\mathrm{u}+v)}-e^{-G_0t}) \\ -H_4((e^{-(\alpha v+\beta w)}-e^{-G_0t})-H_5(e^{-(\mathrm{u}+\alpha v+\beta w)}-e^{-G_0t}) \\ +H_6(e^{-(\mathrm{u}+v)}-e^{-G_0t}))\,\mathrm{r}^2 \end{pmatrix} \quad (16)$$

$$\phi(r,t)=\mathrm{A}_2e^{-wt}-B_2e^{-wt}r^2+\in\begin{pmatrix} M_1(e^{-(\alpha v+\beta w)}-e^{-L_0})^t+M_2(e^{-(\mathrm{u}+\alpha v+\beta w)}-e^{-L_0})^t \\ -M_3((e^{-(\alpha v+\beta w)}-e^{-L_0})^t-M_3(e^{-(\mathrm{u}+\alpha v+\beta w)}-e^{-L_0})^t)\,\mathrm{r}^2 \end{pmatrix} \quad (17)$$

$$p(r,t)=\mathrm{A}_3e^{-qt}-B_3e^{-qt}r^2+\in\begin{pmatrix} N_1(r,t)=N_1(1-e^{-Rt})+N_2(e^{-bt}-e^{-R_0t})+ \\ N_3(e^{-(\mathrm{u}+v)}-e^{-R_0t})-N_4((1-e^{-Rt})+ \\ N_5(e^{-bt}-e^{-R_0t})+N_6(e^{-(\mathrm{u}+v)}-e^{-R_0t}))\,\mathrm{r}^2 \end{pmatrix} \quad (18)$$

Where

$$A=1+\frac{Nu}{2},\mathrm{B}=\frac{Nu}{2},A_1=1+\frac{sh_1}{2},\mathrm{B}_1=\frac{sh_1}{4},A_2=1+\frac{sh_2}{2},\mathrm{B}_2=\frac{sh_2}{4}$$

$$E_1=(-\frac{ba^*}{1+\frac{Nu}{2}})(1+\frac{Nu}{2}),\ E_2=(1+\frac{Nu}{2})\frac{F_1}{F_0},\ E_3=(1+\frac{Nu}{2})\frac{F_2}{(F_0-\alpha b-\beta c)}$$

$$E_4=(1+\frac{Nu}{2})\frac{F_3}{(F_0-a-\alpha b-\beta c)},\ E_5=(1+\frac{Nu}{2})\frac{F_4}{(F_0-a-b)},\ E_6=(\frac{Nu}{2})(\frac{ba^*}{1+\frac{Nu}{2}}),\ E_7=-(\frac{Nu}{2})\frac{F_1}{F_0}$$

$$,\ E_8=-(\frac{Nu}{2})\frac{F_2}{(F_0-\alpha b-\beta c)},\ E_9=-(\frac{Nu}{2})\frac{F_3}{(F_0-a-\alpha b-\beta c)},\ E_{10}=-(\frac{Nu}{2})\frac{F_4}{(F_0-a-b)},$$

$$H_1=(1+\frac{sh_1}{2})\frac{G_1}{(\mathrm{G}_0-\alpha b-\beta c)},\ H_2=(1+\frac{sh_1}{2})\frac{G_2}{(\mathrm{G}_0-a-\alpha b-\beta c)},\ H_3=(1+\frac{sh_1}{2})\frac{G_3}{(\mathrm{G}_0-a-b)},$$

$$H_4=-(\frac{sh_1}{2})\frac{G_1}{(\mathrm{G}_0-\alpha b-\beta c)},\ H_5=-(\frac{sh_1}{2})\frac{G_2}{(\mathrm{G}_0-a-\alpha b-\beta c)},\ H_6=-(\frac{sh_1}{2})\frac{G_3}{(\mathrm{G}_0-a-b)}$$

$$M_1=(1+\frac{sh_2}{2})\frac{L_1}{(\mathrm{L}_0-\alpha b-\beta c)},\ M_2=(1+\frac{sh_2}{2})\frac{L_2}{(\mathrm{L}_0-a-\alpha b-\beta c)},\ M_3=-(\frac{sh_2}{2})\frac{L_1}{(\mathrm{L}_0-\alpha b-\beta c)},$$

$$M_4 = -(\frac{sh_2}{2})\frac{L_2}{(L_0 - a - \alpha b - \beta c)},\ N_1 = (1+\frac{sh_3}{2})\frac{R_1}{R},\ N_2 = (1+\frac{sh_3}{2})\frac{R_2}{R-b},\ N_3 = (1+\frac{sh_3}{2})\frac{R_3}{\mathrm{R-a-b}},$$
$$N_4 = -\frac{sh_3}{2}\frac{R_1}{R},\ N_5 = -\frac{sh_3}{2}\frac{R_2}{R-b},\ N_6 = -\frac{sh_3}{2}\frac{R_3}{\mathrm{R-a-b}}.$$

The computations were done using Maple 17

Result and Discussion

To conclude this analysis we examine the relationship between the Nusselt number (Nu), Lewis number (Le), Sherwood number (Sh), Frank-Kamenetskii number (δ) on the transient state temperature $\theta(r,t)$, the fluid concentration. $\psi(r,t)$, the oxygen concentration $\phi(r,t)$, the average partial pressure of the vapour $\mathrm{p}(r,t)$. Analytical solution given by equation (15)- (18), is computed using computer symbolic algebraic package MAPLE 17. The numerical results obtained from the method are shown in Figure 1 to 4.

Figure 1 depicts the graph of temperature $\theta(r,t)$ against spatial co-ordinate r and time t for different values of Nusselt number Nu. It observed that the temperature decreases with time and decreases along spatial co-ordinate but increases as the Nusselt number increases.

Figure 2 displays the graph of fluid concentration $\psi(r,t)$ against spatial co-ordinate r and time t for different values of Nusselt number Nu. It observed that the fluid concentration decreases with time and decreases along spatial co-ordinate but decreases as the Nusselt number increases.

Figure 3 shows the graph of oxygen concentration $\phi(r,t)$ against spatial co-ordinate r and time t for different values of Nusselt number Nu. It observed that the oxygen concentration decreases with time and decreases along spatial co-ordinate but increases as the Nusselt number increases.

Figure 4 depicts the graph of partial pressure $\mathrm{p}(r,t)$ against spatial co-ordinate r and time t for different values of Nusselt number Nu. It observed that the partial pressure decreases with time and decreases along spatial co-ordinate but decreases as the Nusselt number increases.

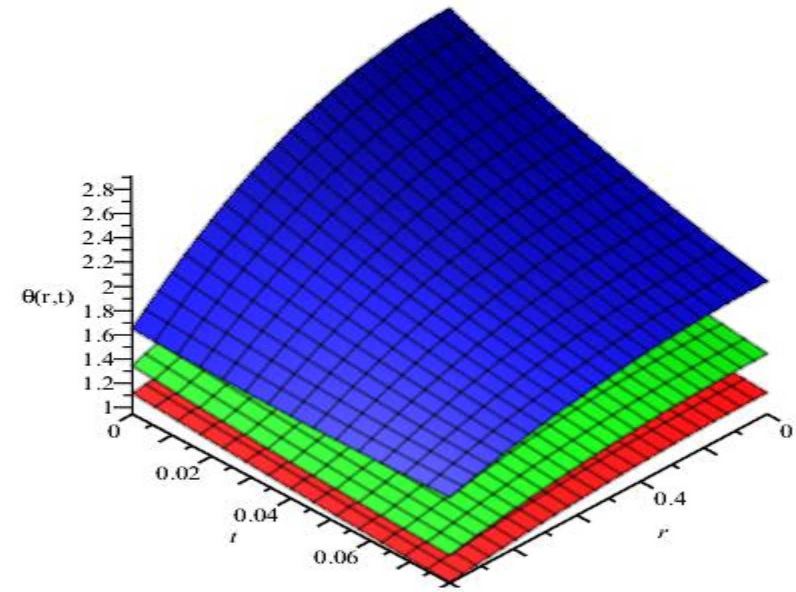

Figure 1: Graph of temperature $\theta(r,t)$ against spatial co-ordinate r and time t for different value of Nusselt number Nu. Nu=1 (read), Nu=2(Green) and Nu=4 (Blue)

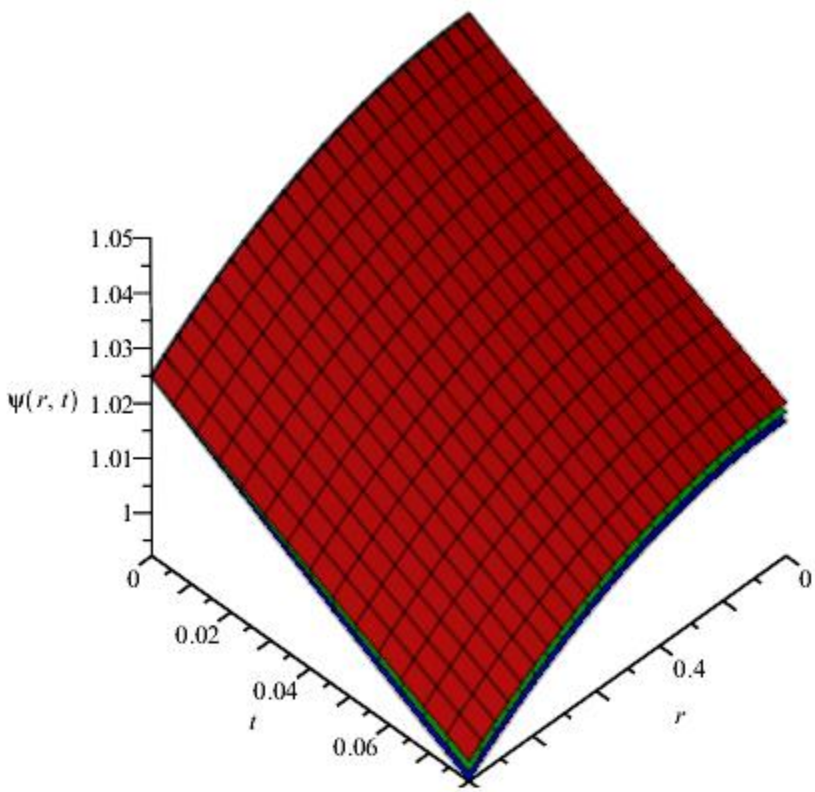

Figure 2: Graph of fluid concentration $\psi(r,t)$ against spatial co-ordinate r and time t for different value of Nusselt number Nu. Nu=1 (read), Nu=2(Green) and Nu=4 (Blue)

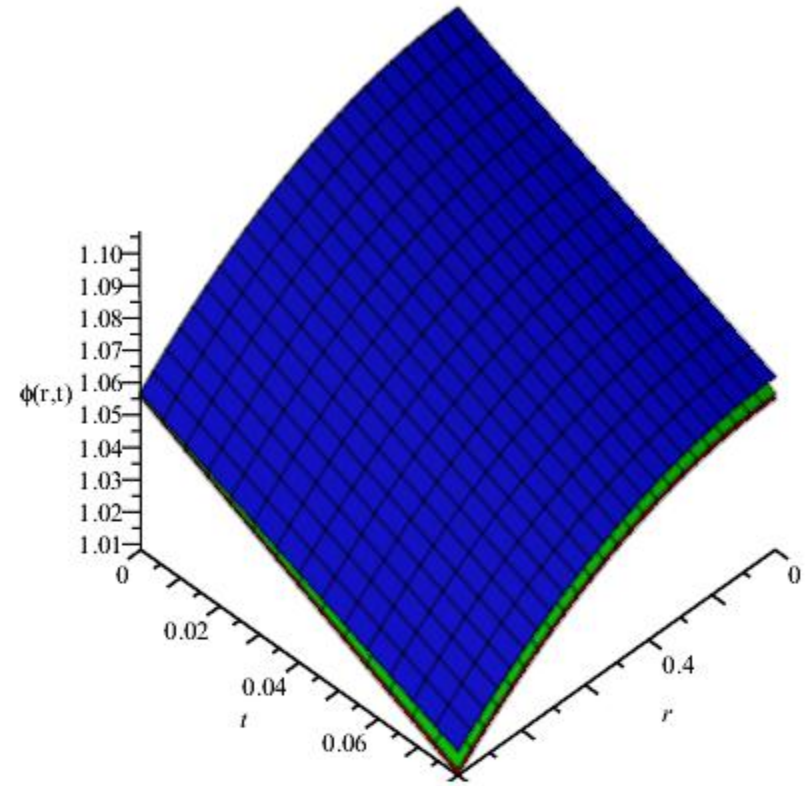

Figure 3: Graph of oxygen concentration $\phi(r,t)$ against spatial co-ordinate r and time t for different value of Nusselt number Nu. Nu=1 (read), Nu=2(Green) and Nu=4 (Blue)

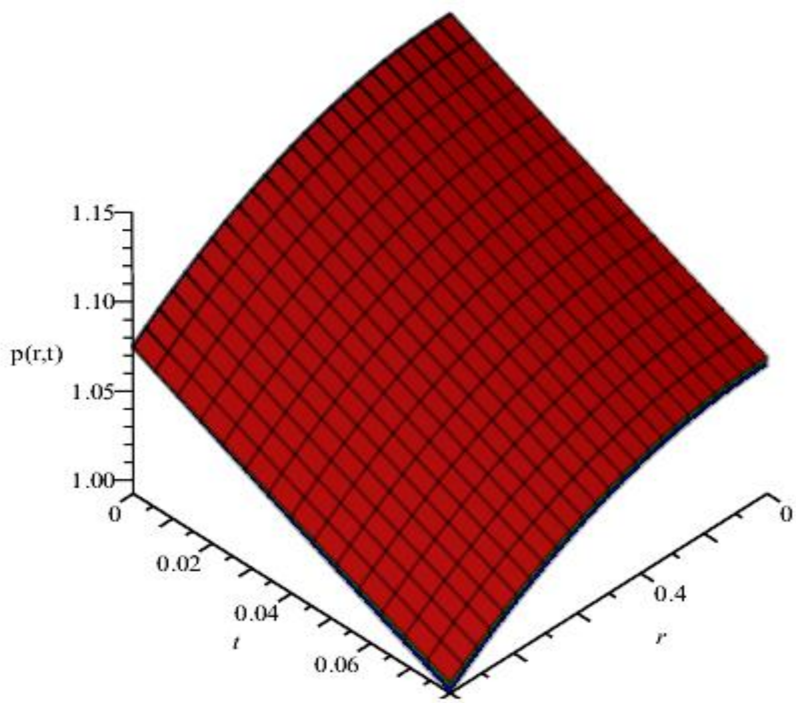

Figure 4: Graph of partial pressure $p(r,t)$ against spatial co-ordinate r and time t for different value of Nusselt number Nu. Nu=1 (read), Nu=2(Green) and Nu=4 (Blue)

It is worth pointing out that the effects observed in figure 1-4 are important to guide insulation materials manufactures so as to provide safety precaution during storage and usage.

Conclusion

For a high activation energy situation (i.e. as $\in \longrightarrow \mathbf{O}$), we have solved the equations governing the auto ignition of combustible fluid in insulation materials incorporating partial pressure of the vapour and heat transfer at surface analytically using polynomial approximation method. From the result obtained, we can conclude that, Nusselt number enhanced the medium temperature and oxygen concentration while it decrease the fluid concentration and partial pressure of vapour.

The results obtained are not only expected to guide manufacturers of insulation materials but provide safety precautions during storage and usage.

References

Aziz Hairuddin, A., Wandel, A. P., & Yusaf, T. (2013). Effect of different heat transfer models on a diesel homogeneous charge compression ignition engine. *International Journal of Automotive and Mechanical Engineering,* 8, 1292-304.

Chen, Z., Yao, M. F., Zheng, Z. Q., Zhang, B., & Xing, Y. (2006). Optimal strategy for HCCI combustion of dual-fuel*. Ranshao Kexue Yu Jishu/Journal of Combustion Science and Technology,* 12, 142-6.

Firmansyah, A. A., & Heikal, M. R. (2013). Double stage wiebe: An approach to single zone modeling of dual fuel HCCI combustion. *Asian Journal of Scientific Research,* 6, 388-94.

Kamil, M., Rahman, M. M., & Bakar, R. A. (2014). An integrated model for predicting engine friction losses in internal combustion engines. *International Journal of Automotive and Mechanical Engineering,* 9, 1695-708.

Kocher, L.E., Hall, C. M., Stricker, K., Fain, D., Alstine, D., & Shaver, G. M. (2014). Robust oxygen fraction estimation for conventional and premixed charge compression ignition engines with variable valve actuation. *Control Engineering Practice,* 29, 187-200.

Krasselt, J., Foster, D., Ghandhi, J., Herold, R., Reuss, D., & Najt, P. (2009). Investigations into the effects of thermal and compositional stratification on HCCI combustion – Part I: metal engine results. *SAE International Journal Engines,* 2, 1034-53.

Lu, X., Hou, Y., Zu, L., Huang, Z., & Lü, X. V. (2009). Experimental study on the auto-ignition and combustion characteristics in the homogeneous charge compression ignition (HCCI) combustion operation with ethanol/n-heptane blend fuels by port injection. *Fuel. X,* 85, 2622-31.

Saxena, S., & Bedoya, I. D. (2013). Fundamental phenomena affecting low temperature combustion and HCCI engines, high load limits and strategies for extending these limits. *Progress in Energy and Combustion Science*, 39,457-88.